2016

Investigations Of Low Pressure Two-Phase Steam-Water Injector

Roman Kwidzinski
Institute of Fluid-Flow Machinery Polish Academy of Sciences,ul. Gen. J. Fiszera 14, Gda?sk , 80-231, Poland, rk@imp.gda.pl

Dariusz Butrymowicz
Bialystok University of Technology, Faculty of Mechanical Engineering, Wiejska 45C, Bialystok, Poland, d.butrymowicz@pb.edu.pl

Jaroslaw Karwacki
Institute of Fluid-Flow Machinery Polish Academy of Sciences,ul. Gen. J. Fiszera 14, Gda?sk , 80-231, Poland, jkarwacki@imp.gda.pl

Marian Trela
Institute of Fluid-Flow Machinery Polish Academy of Sciences,ul. Gen. J. Fiszera 14, Gda?sk , 80-231, Poland, mtr@imp.gda.pl

Kamil Smierciew
Bialystok University of Technology, Faculty of Mechanical Engineering, Wiejska 45C, Bialystok, Poland, k.smierciew@pb.edu.pl

Investigations of Low Pressure Two-Phase Steam–Water Injector

Roman KWIDZIŃSKI[1], Dariusz BUTRYMOWICZ[2]*, Jarosław KARWACKI[1],
Marian TRELA[1], Kamil ŚMIERCIEW[2]

[1] The Szewalski Institute of Fluid-Flow Machinery Polish Academy of Sciences,
ul. Gen. J. Fiszera 14, 80-231 Gdańsk, Poland
roman.kwidzinski@imp.gda.pl

[2]Bialystok University of Technology, Faculty of Mechanical Engineering,
ul. Wiejska 45C, 15-351 Białystok, Poland
d.butrymowicz@pb.edu.pl

* Corresponding Author

ABSTRACT

Steam–water injector is a passive device used to compress and heat a stream of cold water. Recently such injectors found new applications in thermal engineering, refrigeration and air conditioning, e.g. low pressure steam–water injector may be applied as a thermal driven liquid pump in absorption and steam ejection refrigeration systems. In this paper a close attention is paid to steam–water injectors in which superheated steam of relatively low pressure is the driving medium. Selected results of experimental and theoretical studies of a such type of injector are presented. Experimental research was conducted on a laboratory scale injector made of transparent material. The measured parameters included the pressure and temperature distributions in the injector as well as inlet mass flow rates of both fluids during the injector stable operation. Between the measurements, inlet water flow rate and/or outlet back-pressure varied. On this basis experimental flow characteristics of the injector were determined. In theoretical part of the study, recorded distributions of pressure and temperature in the injector mixing chamber were used to evaluate the heat transfer coefficient during condensation in the mixing chamber. A new correlation predicting the Nusselt number for the heat transfer in the mixing chamber is also presented.

1. INTRODUCTION

Vapor–liquid injector is a passive device in which thermal energy of vapor is used to compress and heat a cold liquid. In the past such injectors were used extensively for feeding water into boilers, especially of steam engines. Recently an interest in the two-phase injectors revived with new proposals of their application in thermal engineering (Ohmori *et al.*, 2007), air conditioning and refrigeration (Chen *et al*., 2013; Śmierciew *et al.*, 2015).

Steam–water injectors may be applied as thermal driven liquid pumps in absorption LiBr systems as well as in steam ejection systems, as it is shown in Fig. 1 and Fig. 2. The general motivations of application of the two-phase injector instead of a mechanical pump in these systems are:

- two-phase injector is driven by part of steam that is generated already in the system; in this case the refrigeration system is fully thermal driven, without any consumption of electric power to drive the system;
- two-phase injector operates as a pre-heater of water supplied to the steam generator improving the system efficiency;
- this type of injector is more simple and reliable than mechanical liquid pump because it has no moving parts and is not influenced to possible cavitation that may occur in mechanical pumps.

In this paper close attention is paid to steam-water injectors in which superheated steam of relatively low pressure is the driving medium. The steam is expanded and accelerated to a near-sonic velocity in a convergent steam nozzle

(SN), Fig. 3. Leaving the nozzle, it enters the mixing chamber (MC), creating there a low static pressure sufficient for water to be drawn into the MC through an annular slot (gap) surrounding the SN exit. Both phases – having different temperatures and velocities – exchange mass, momentum and energy in the mixing chamber during condensation of vapor at a contact surface with the liquid (water). Resulting two-phase flow is compressed in a condensation wave developing in diffuser (DF) downstream of the throat. Inside the wave region the flow velocity decreases substantially as the vapor phase completely condenses. Thus only liquid water is leaving the injector at a pressure that – in some conditions – could exceed the pressure of the motive steam.

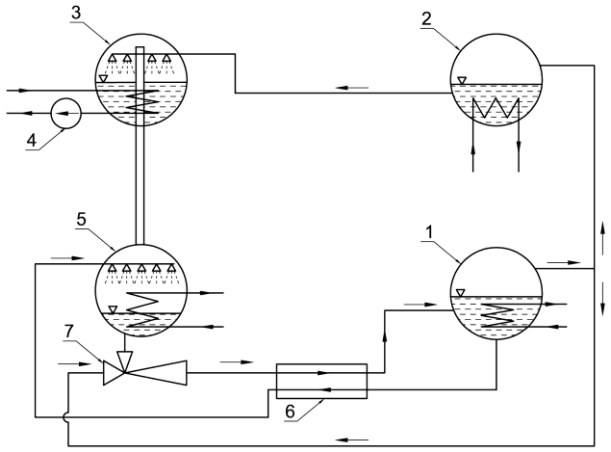

Figure 1: Modified absorption LiBr refrigeration system with two-phase injector as a liquid pump: 1– steam generator; 2 – condenser; 3 – evaporator; 4 – cold water pump; 5 – absorber; 6 – internal heat exchanger; 7 – steam-water injector.

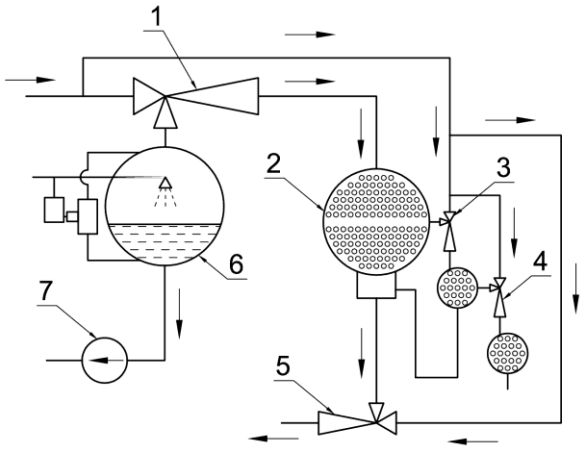

Figure 2: Modified steam ejection refrigeration system with two-phase injector as a liquid pump: 1– motive ejector; 2 – condenser; 3 – ejector vacuum pump of 1st step; 4 – ejector vacuum pump of 2nd step; 5 – steam-water injector; 6 – evaporator; 7 – cold water pump.

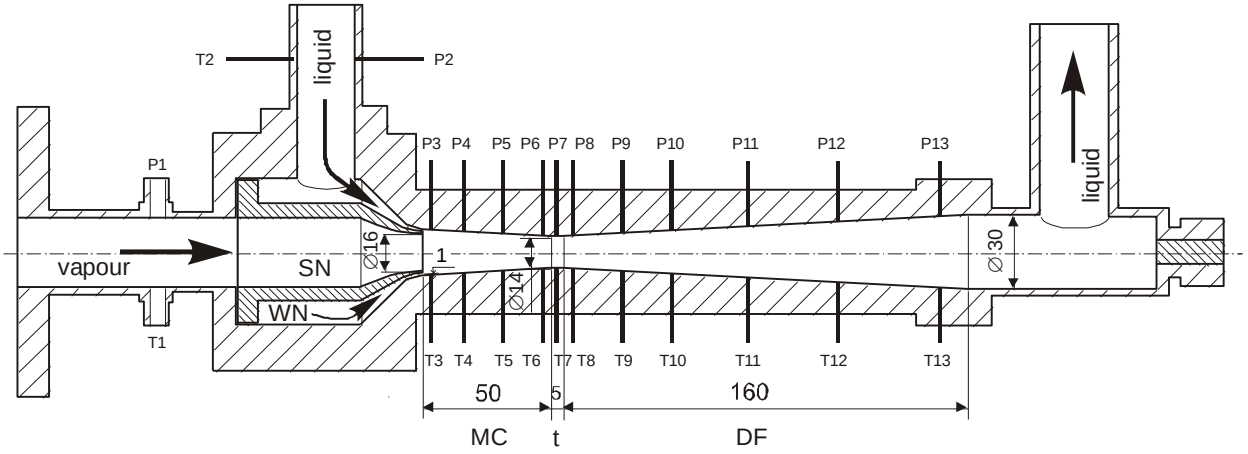

Figure 3: Schematic and principal dimensions of the investigated low pressure steam–water injector: SN – steam nozzle, WN – water nozzle, MC – mixing chamber, DF – diffuser, t – throat, T1 - T13 – temperature measurement, P1 - P13 – pressure measurement.

Two-phase injectors are usually applied as a jet pump or a heater. In the injector working as a jet pump it is important to ensure that thermodynamic process in it results in as high exit pressure as possible without losing the flow stability. This paper presents results of the experimental investigations of stable injector operation and focus on its maximum discharge pressure and heat transfer in its mixing chamber. The investigated injector was designed to work with relatively low pressure motive steam, which enters the mixing chamber with near-critical (-sonic) velocity. Such operating conditions may be applied in the cases of refrigeration systems showed in Fig. 1 and Fig. 2.

The presented results are a part of research of two-phase injectors conducted at IFFM in Gdańsk, and can be connected with the previous studies of supercritical steam injectors, see for example Kwidziński and Trela (2007).

2. EXPERIMENTAL INVESTIGATION

Experimental investigations of the low-pressure steam–water injector (LPSI) were conducted on a laboratory scale injector designed and built at the Szewalski Institute of Fluid-Flow Machinery of the Polish Academy of Sciences. The mixing chamber and diffuser of the injector were made of transparent material to allow for visual inspection of the two-phase flow structures. Principal dimensions of the investigated LPSI are given in Fig. 3.

Schematic view of the experimental stand used is shown in Fig. 4. The stand is equipped with the supply lines for steam (motive fluid) and water (secondary fluid). The LPSI 1 is driven by a steam supplied by the steam generator 3 through a separator 4 and superheater 5. Water is pumped to LPSI by the pump 6 for better control of the flow rate, not sucked in as in real conditions. The water flowing out of the LPSI fills the tank 2 from where it is directed back to the injector. Its temperature is kept constant (typically at 15 °C) with the help of cooler 7. Excess of the water returns to the steam generator. Control valves 10 and 11 are used to adjust the inlet pressures of steam and water. The valve 12 installed downstream of the LPSI is used to set the back-pressure.

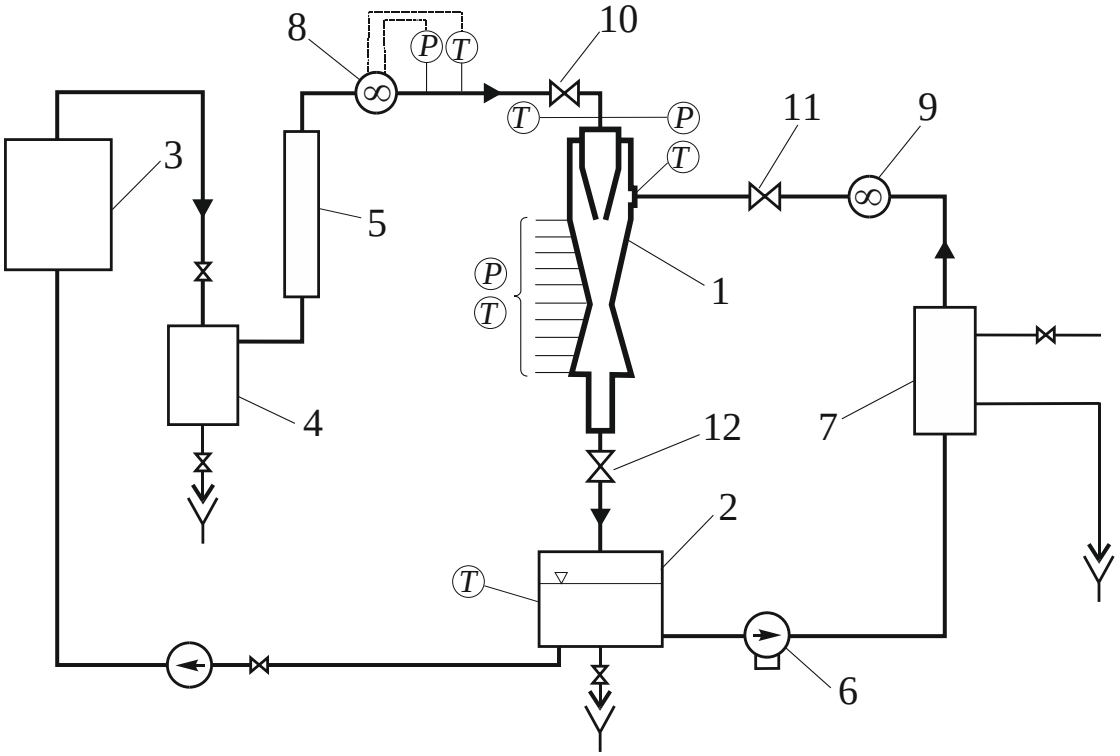

Figure 4: Schematic diagram of the experimental stand: 1 – low pressure steam-water injector, 2 – water tank, 3 – steam generator, 4 – steam separator, 5 – steam superheater, 6 – water pump, 7 – water cooler, 8 – steam flow meter, 9 – water flow meter, 10 – steam pressure control valve, 11 – water flow control valve, 12 – back-pressure control valve.

The parameters measured and recorded during the LPSI tests included distributions of average pressure and temperature along the mixing chamber and diffuser walls. Also, inlet steam and inlet water flow rate, pressure and temperature were recorded. Location of the measurement points is depicted in Fig. 3. Pressure was measured by piezoelectric transducers with accuracy class of 0.1. K-type thermocouples were used for temperature measurement. Steam mass flow rate was measured with accuracy 1.25 % by vortex flow meter 8; Coriolis flow meter 9 was used to measure the water mass flow rate with accuracy 0.5 %. Measured parameters were recorded by digital acquisition system with frequency 2 Hz and then averaged if necessary.

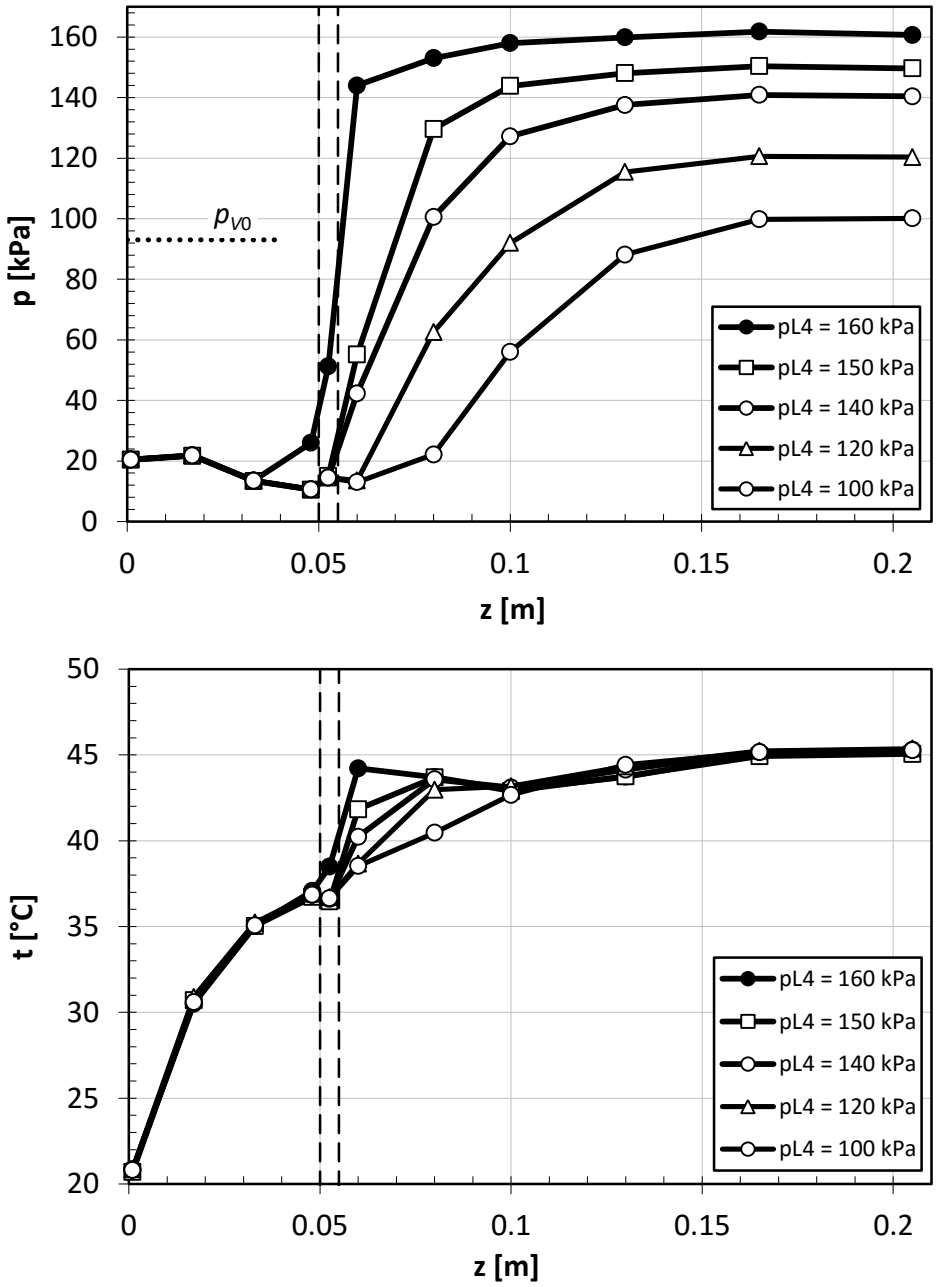

Figure 5: Distributions of average pressure p and temperature t along the LPSI mixing chamber and diffuser wall measured for constant inlet flow parameters and selected values of back-pressure p_{L4}. Dashed lines indicate the extent of cylindrical throat. Inlet steam parameters: pressure 93 kPa (shown in pressure diagram as p_{V0}), mass flow rate 111 kg/h, superheating 27 ºC. Inlet water parameters: temperature 20 °C, mass flow rate 2670 kg/h.

Experimental investigation of the LPSI steady flow characteristics included the measurements of pressure and temperature along the mixing chamber and diffuser for constant inlet flow parameters. Between the measurements of the inlet water flow rate could be varied in a range from 1500 kg/h to 3600 kg/h. The back pressure was also adjusted up to a value when a condensation wave approached the mixing chamber throat. During the back-pressure changes, the position where condensation completes was observed visually in the diffuser. This position is easy to observe because the flow changes from white two-phase mixture to transparent liquid water at well-defined channel cross-section.

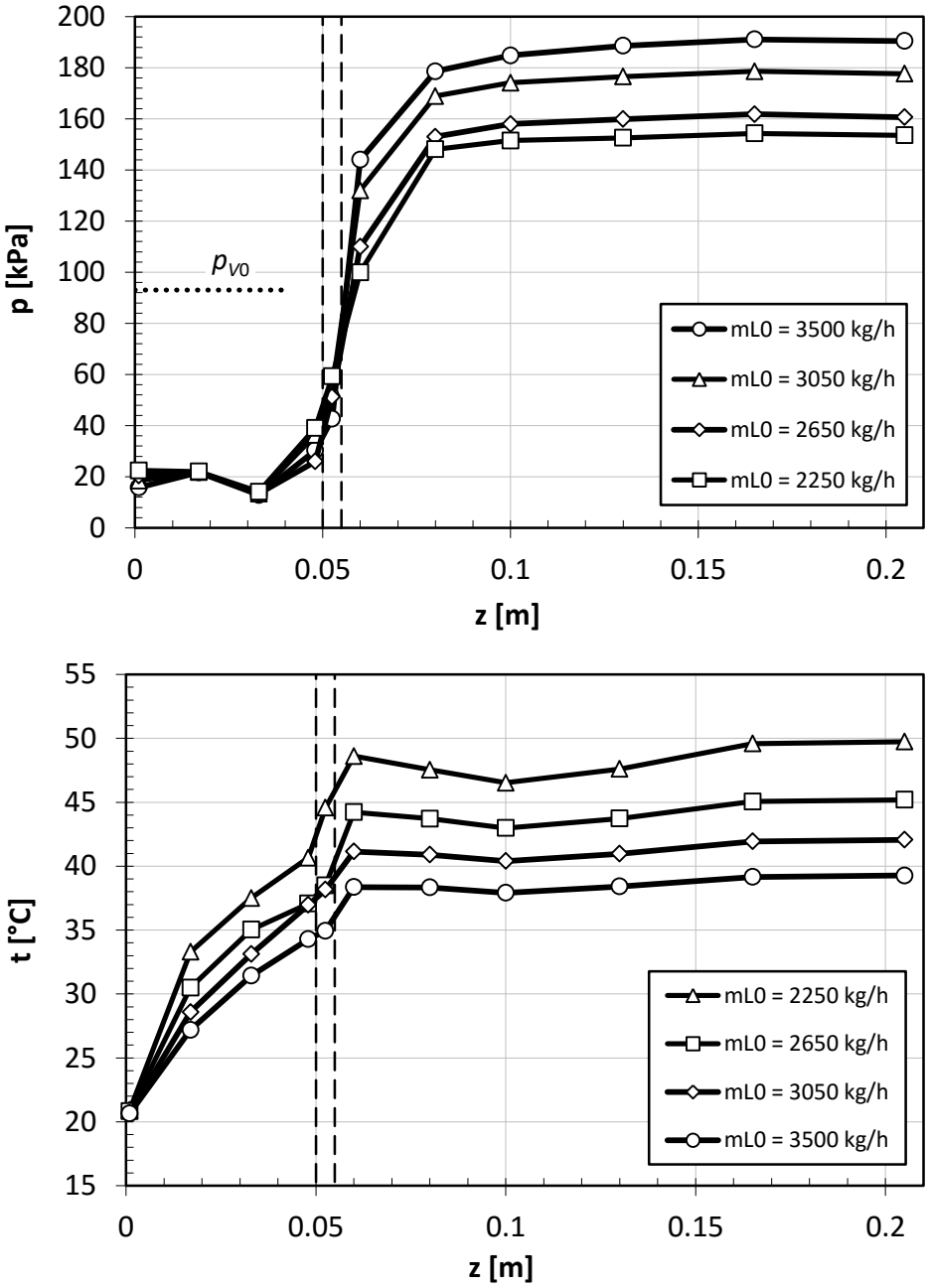

Figure 6: Distributions of average pressure p and temperature t along the LPSI mixing chamber and diffuser wall measured for three selected water flow rates $\dot{m}_{L0}$ at near-maximum back-pressure. Dashed line indicates the extent of cylindrical throat. Inlet steam parameters: pressure 93 kPa (shown in pressure diagram as p_{V0}), mass flow rate 111 kg/h, superheating 26 ºC. Inlet water temperature 20 °C.

Exemplary results of pressure p and temperature T measurements are shown in Fig. 5 and Fig. 6. The profiles of pressure and temperature recorded during the research are typical for a steam–water injector. Rapid pressure rise is observed in the condensation wave region followed by further, moderate increase along the diffuser.

Two facts are worth of note. Firstly, the change of pressure in the diffuser propagates upstream of the condensation wave, so the two-phase flow in the mixing chamber is subcritical. Secondly, the exit pressure exceeds the inlet vapor pressure for sufficiently high water-to-vapor mass flow ratio, which is essential in application of a steam injector as

a pump. For lower values of water flow rate, the exit pressure diminishes but higher water temperature rise is gained; in this mode the injector can operate as a heat exchanger. Even higher temperature rise can be achieved when the outlet pressure is lowered further, which results in the downstream shift of the condensation wave and extension of two-phase flow region where condensation heat transfer takes place.

Figure 5 illustrates the changes of pressure and temperature profiles when the back-pressure is raised. In this case the condensation wave moves upstream of the diffuser. It can be seen that the average temperature profiles are practically independent of the back-pressure value. Discrepancies seen in the region of condensation wave result from the oscillations of condensation terminus inside the wave region. For fixed inlet flow parameters, maximum back-pressure is reached when the wave is located immediately downstream of the mixing chamber throat. Any further rise of back-pressure will result in a loss of two-phase flow stability and interruption of the injector pumping action.

The maximum back-pressure depends on the inlet flow conditions. Figure 6 shows exemplary results for LPSI operating under near-maximum back-pressure and various inlet water flow rates; the motive steam parameters are constant in this case. In can be noted that the outlet water temperature decreases with the increase of inlet water flow rate while the outlet pressure rises. Figure 7 shows the LPSI maximum back-pressure in dimensionless form as a function of compression ratio versus entrainment ratio. The compression ratio is defined here as:

$$\Pi = \frac{p_{L4} - p_{L0}}{p_{V0} - p_{L0}} \tag{1}$$

and the entrainment ratio is:

$$U = \frac{\dot{m}_{L0}}{\dot{m}_{V0}}. \tag{2}$$

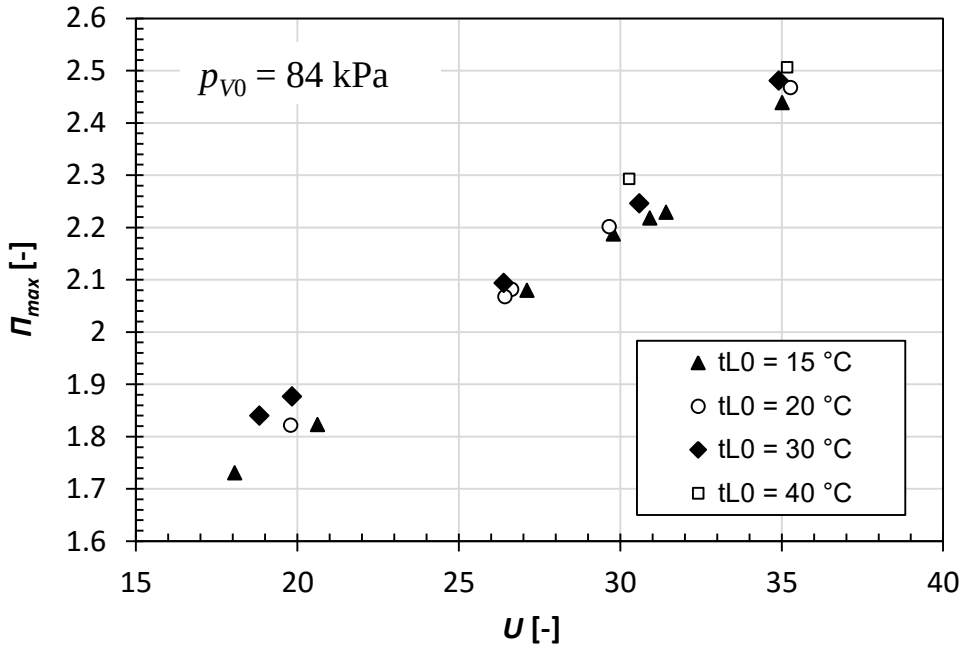

Figure 7: Compression ratio Π as a function of entrainment ratio U calculated for the LPSI driven by a steam at pressure p_{V0} = 84 kPa, flow rate 100 kg/h and superheating 26 ºC. Inlet water temperature t_{L0} was in the range 15 - 40 °C.

Compression ratio values depicted in Fig. 7 were obtained for the LPSI working with fixed motive steam pressure of 84 kPa and flow rate of 100 kg/h and different inlet water temperatures in the range 15 - 40 °C. In such conditions the compression ratio rises with increase of inlet water flow rate. For a given *U*, the compression ratio slightly drops with the increasing inlet water temperature. Highest compression ratio achieved for the mentioned inlet parameters was equal to 2.5. Investigations performed under different values of motive steam pressure indicated that the compression ratio rises with this pressure. For example, for p_{V0} = 128 kPa and U = 35 a value of Π = 2.7 was achieved.

3. EVALUATION OF HEAT TRANSFER COEFFICIENT

Average heat transfer coefficient for condensation in the LPSI mixing chamber was calculated from experimental data following the procedure developed by Dumaz and Duc (1999). It is assumed that semi-annular flow is present in the major part of the mixing chamber so the heat transfer area and the chamber wall area are comparable. Also, as liquid phase is present at the wall along the entire mixing chamber length, water properties can be calculated from pressure and temperature measured at the wall. Steam is assumed to remain saturated during the condensation so its properties depend on the measured static pressure only. Taking above into account it is possible to write down a definition of the average heat transfer coefficient α in the mixing chamber as

$$\alpha = \frac{\dot{m}_c h_{LV}}{A \Delta \overline{T}}, \tag{3}$$

where: $\dot{m}_c$ is condensate mass flow rate, h_{LV} – latent heat of condensation, A – surface area of the mixing chamber wall, $\Delta \overline{T}$ – logarithmic mean temperature difference between the vapor and liquid in the mixing chamber. The condensate mass flow $\dot{m}_c$ can be found from energy balance equation in the control volume comprising entire mixing chamber,

$$\dot{m}_{V0} h_{V1,sat} + \dot{m}_{L0} h_{L1} = (\dot{m}_{L0} + \dot{m}_c) h_{L2} + (\dot{m}_{V0} - \dot{m}_c) h_{V2,sat}. \tag{4}$$

After simple transformation one gets from (4) the following relation for the mass flow of condensed steam:

$$\dot{m}_c = \frac{\dot{m}_{V0}(h_{V1,sat} - h_{V2,sat}) + \dot{m}_{L0}(h_{L1} - h_{L2})}{h_{L2} - h_{V2,sat}}. \tag{5}$$

Values of the average heat transfer coefficient α calculated from the experimental data recorded during LPSI tests were in the range of 0.4 to 1 MW/m^{2}K and are shown in Fig. 8. They are approximately 50 % larger than α evaluated for a similar steam injector but driven by a steam of higher pressure (~350 kPa), expanded to a supercritical (supersonic) velocity, which was investigated previously by the authors (see Trela *et al*. 2004).

The "experimental" values of the average heat transfer coefficient α were used to formulate a correlation of the Nusselt number for heat transfer in the LPSI mixing chamber. The correlation is based on an analysis of 1D two-fluid model of the flow in vapor-liquid injector mixing chamber that is outlined in Trela & Kwidziński 2003. It relates the Nusselt number to a set of dimensionless parameters and for the LPSI takes a form

$$\mathrm{Nu} = 0.18\, \mathrm{Re}_{V1}^{1.04}\, U^{0.25}\, S_1^{0.17}\, \mathrm{Oh}_{L1}^{0.43}. \tag{6}$$

In the above correlation, the Nusselt number is based on the steam nozzle outlet diameter,

$$\mathrm{Nu} = \frac{\alpha D_{V1}}{\lambda_{L1}}. \tag{7}$$

The Reynolds number also refers to the steam at the nozzle outlet,

$$\mathrm{Re}_{V1} = \frac{4 \dot{m}_{V0}}{\pi D_{V1} \mu_{V1,sat}}, \tag{8}$$

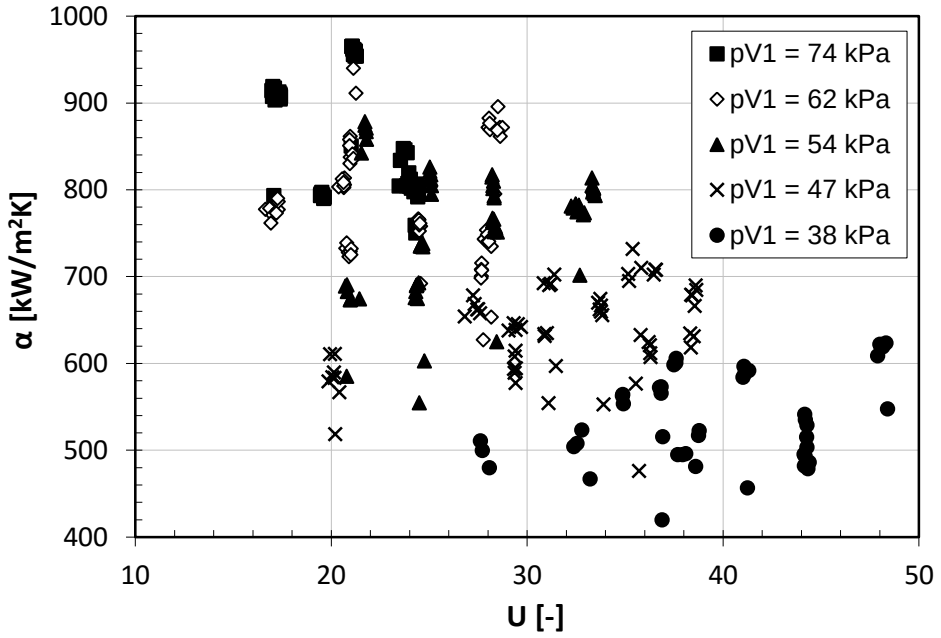

Figure 8: Average heat transfer coefficient α calculated from pressure and temperature distributions in the LPSI mixing chamber. The points are grouped by mixing chamber inlet pressure p_{V1}.

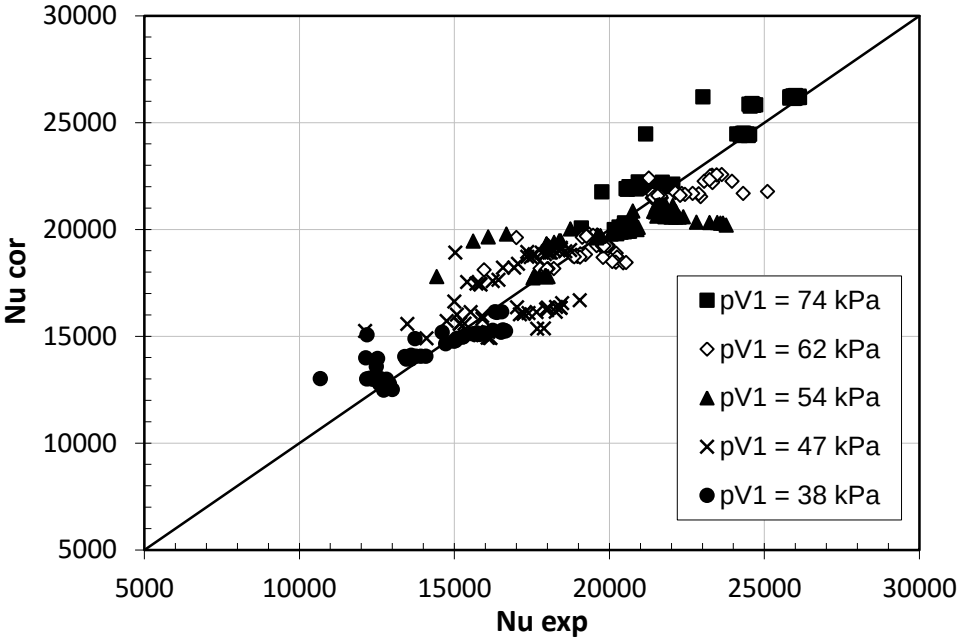

Figure 9: Correlated (6) vs experimental average heat transfer coefficient α for LPSI mixing chamber. The points are grouped by mixing chamber inlet pressure p_{V1}.

while the Ohnesorge number is calculated for the liquid parameters at the water nozzle outlet,

$$Oh_{L1} = \frac{\mu_{L1}}{\sqrt{\rho_{L1}\sigma_{L1}\delta_{L1}}}, \tag{9}$$

where δ_{L1} denotes the width of water nozzle gap. The remaining two parameters are entrainment ratio U and velocity ratio,

$$S_1 = \frac{w_{V1}}{w_{L1}}, \tag{10}$$

at the mixing chamber inlet. The correlation is valid within the parameter ranges

$$137000 < \mathrm{Re}_{V1} < 263000,\ 16 < U < 49,\ 24 < S_1 < 44,\ 0.0024 < \mathrm{Oh}_{L1} < 0.0045,$$

with the correlation coefficient equal to $R = 0.878$.

4. CONCLUSIONS

In the paper flow characteristics of a low pressure steam-water injector (LPSI) has been presented. Based on the results of the authors experimental research it was found that the profiles of pressure and temperature in the LPSI are typical for a vapor–liquid injector of the central motive nozzle arrangement. The principal pressure gain of the liquid stream in such injectors takes place in a region of condensation wave which forms in diffuser close to the mixing chamber throat, see Fig. 6. During the reported experiments with LPSI, the highest observed compression ratio Π reached about 2.5, see Fig. 7. In this case the discharge to motive pressure ratio, p_{L4}/p_{V0}, was approximately 2.2.

In theoretical part of the paper, attention was paid to the evaluation of heat transfer coefficient α during condensation in the LPSI mixing chamber. The values of α evaluated according to eq. (3) are relatively high for the steam injectors. For the LPSI they reach 1 MW/m^{2}K, see Fig. 8. In comparison to the previously investigated supercritical steam injectors, they are higher by about 50 %.

NOMENCLATURE

A	surface area	(m^2)
D	diameter	(m)
h	specific enthalpy	(J/kg)
$\dot{m}$	mass flow rate	(kg/s)
p	pressure	(Pa)
T	temperature	(ºC, K)
U	entrainment ratio	(–)
w	velocity	(m/s)

Greek letters

α	average heat transfer coefficient in the mixing chamber	(W/m^{2}K)
δ	width of the water nozzle gap	(m)
λ	thermal conductivity	(W/m·K)
μ	dynamic viscosity	(Pa·s)
ρ	density	(kg/m^3)
σ	surface tension	(N/m)
Π	compression ratio	(–)

Subscript

c	condensation
L	liquid
sat	at saturation
V	vapor
0	steam injector inlet
1	mixing chamber inlet
2	mixing chamber outlet
4	steam injector outlet

REFERENCES

Chen, X., Omer, S., Worall, M., Riffat, S. (2013). Recent developments in ejector refrigeration technologies. *Renew. Sust. Energy Rev., 19*, 629–651.

Dumaz, P., Duc, B. (1999). The DIVA program: Some experimental results and first CATHARE calculations. *Proceedings of The 9th Int. Topical Meeting on Nuclear Reactor Thermal Hydraulics (NURETH-9), San Francisco, CA* (CD-ROM, 12 pages). La Grange Park, IL: American Nuclear Society.

Kwidziński, R., Trela, M. (2007). Investigation of steam injector with variable throat cross-section, *Arch. Thermod., 28*(1), 3–14.

Ohmori, S., Narabayashi, T., Mori, M., Iwaki, Ch., Asanuma, Y., Goto, Sh. (2007). Development of technologies on innovative-simplified nuclear power plant using high-efficiency steam injectors – System outline and endurance test of low-pressure steam injectors. *J. Power & Energy Syst., 1*(1), 99–110.

Śmierciew, K., Butrymowicz, D., Kwidziński, R., Przybyliński, T. (2015). Analysis of application of two-phase injector in ejector refrigeration systems for isobutane. *Appl. Therm. Eng.*, 78, 630–639.

Trela, M., Butrymowicz, D., Dumaz, P. (2004). Experimental investigations of heat transfer in steam-water injector. *Proceedings of 5th International Conference on Multiphase Flow (ICMF'04), Yokohama, Japan* (CR-ROM, Paper No. 544).

Trela, M., Kwidziński, R. (2003). Modelling of physical phenomena in supercritical two-phase steam injector. *Arch. Thermod*., 24(4), 15–34.

ACKNOWLEDGEMENT

This work was supported by Polish state budget through a research project No N513 485239.